Interferometric measurement of femtosecond wave-packet tilting in rutile crystal

C. Radzewicz

Department of Electrical and Computer Engineering and Center for Laser Research, Oklahoma State University, Stillwater, Oklahoma 74078 and Institute of Experimental Physics, University of Warsaw, Warsaw, Poland

J. S. Krasinski and M. J. la Grone

Department of Electrical and Computer Engineering and Center for Laser Research, Oklahoma State University, Stillwater, Oklahoma 74078

M. Trippenbach and Y. B. Band

Department of Chemistry and Department of Physics, Ben-Gurion University, Beer Sheva, Israel

Received March 13, 1996; revised manuscript received June 17, 1996

We measured the tilting of a femtosecond laser wave packet in a birefringent rutile crystal. The measurements were carried out with a linear interferometric technique that, in contrast to nonlinear correlation techniques, allows measurement at very low power. A 23-fs delay between the left and the right parts of a 30-fs, 800-nm wave packet with 20° divergence was measured for a 1-mm-thick rutile crystal, in agreement with theoretical predictions. © 1997 Optical Society of America [S0740-3224(97)00702-9]

PACS number(s): 42.25.−p, 42.25.Bs, 42.25.Lc

Theoretical analysis of an optical wave packet (WP) propagating as an extraordinary wave in a nonisotropic dispersive medium recently led to the prediction of rotation (or tilt) of the WP about an axis perpendicular to the propagation vector.[1] However, experimental evidence for such an effect has never been presented. Such tilting can have significant consequences for both linear and nonlinear optical phenomena. For example, in type II sum-frequency generation or second-harmonic generation $[o(\omega_1) + e(\omega_2) \rightarrow o(\omega_3)]$, the ordinary and the extraordinary input WP's can become nonoverlapping because of the extraordinary wave-packet tilt (in addition to walk-off). In type I sum-frequency generation or second-harmonic generation $[o(\omega_1) + o(\omega_2) \rightarrow e(\omega_3)]$ the output WP can tilt relative to the input WP's, thus preventing reconversion in the strong conversion limit. In the case of a radio-wave pulse propagating through the ionosphere, the anisotropy that is due to the presence of the earth's magnetic field can tilt the pulse, thus affecting interferometric measurements of radio-wave signals arriving at earth. Here we present the first, to our knowledge, experimental evidence of wave-packet tilting in nonisotropic dispersive media.

The propagation equation for the slowly varying envelope $A(\mathbf{x}, t)$ of the electric field in a nonisotropic dispersive medium with index of refraction $n(\omega, \mathbf{s})$, where ω is the light frequency and $\mathbf{s}$ is the unit vector in the propagation direction, is given by the following form:

$$\frac{\partial}{\partial z} A(\mathbf{x}, t) = \left(-\beta_1 \frac{\partial}{\partial t} - \frac{i}{2} \beta_2 \frac{\partial^2}{\partial t^2} + \frac{1}{6} \beta_3 \frac{\partial^3}{\partial t^3} + \cdots + \gamma_x \frac{\partial}{\partial x} + \gamma_y \frac{\partial}{\partial y} - \frac{i}{2} \gamma_{xx} \frac{\partial^2}{\partial x^2} - \frac{i}{2} \gamma_{yy} \frac{\partial^2}{\partial y^2} + i \gamma_{xt} \frac{\partial}{\partial x} \frac{\partial}{\partial t} + i \gamma_{yt} \frac{\partial}{\partial y} \frac{\partial}{\partial t} + i \gamma_{xy} \frac{\partial}{\partial x} \frac{\partial}{\partial y} \cdots \right) A(\mathbf{x}, t). \quad (1)$$

Here the propagation vector for the central component of the field, $\mathbf{k}_0$, is along z. The dispersion parameters β_1, β_2, β_3, correspond to the inverse group velocity, the group-velocity dispersion, and higher-order dispersion, respectively. The $\gamma_x(\gamma_y)$ terms describe walkoff [the ratios of the $x(y)$ component to the z component of the group velocity]; γ_{xx} and γ_{yy} are generalized Fresnel diffraction coefficients, which depend on the derivatives of the index of refraction with respect to direction $\mathbf{s}_0$ (the unit vector along $\mathbf{k}_0$). The γ_{xy} term rotates the amplitude of the WP in the x–y plane. The γ_{xt} and γ_{yt} terms of Eq. (1) are responsible for a number of different effects, one of which involves rotation of the amplitude of the WP about the y and x axes, respectively, and modifies the phase fronts to be parabolic. Explicit expressions for the coefficients in Eq. (1) are given in Ref. 1. For a uniaxial crys-

tal, γ_y, γ_{yt}, and γ_{xy} vanish in the coordinate system in which the optic axis is in the $x-z$ plane, but the amplitude of the WP is tilted about the y axis because of the γ_{xt} term.

Figure 1(a) schematically shows the propagation of a WP in a positive uniaxial crystal. The initial WP with average wave vector along the z axis is shown on the left. Upon propagating through the crystal, the rays at a given frequency with direction closer to the optic axis have a higher velocity than those with direction farther from the optic axis. Therefore the WP rotates clockwise and the center of the WP walks off the z axis. Also, the temporal duration of the WP is increased owing to group-velocity dispersion, and the size of the WP in directions perpendicular to z is increased owing to Fresnel diffraction upon propagation through the medium.

To demonstrate tilting of the WP, we carried out experiments with birefringent positive uniaxial rutile (TiO_2) crystals.[2] As shown in Fig. 1(b), the light beam is focused in the crystal, but because of the presence of lenses L1 and L2, the beam is recollimated outside of the crystal. The wave-packet tilt is preserved in the collimated output

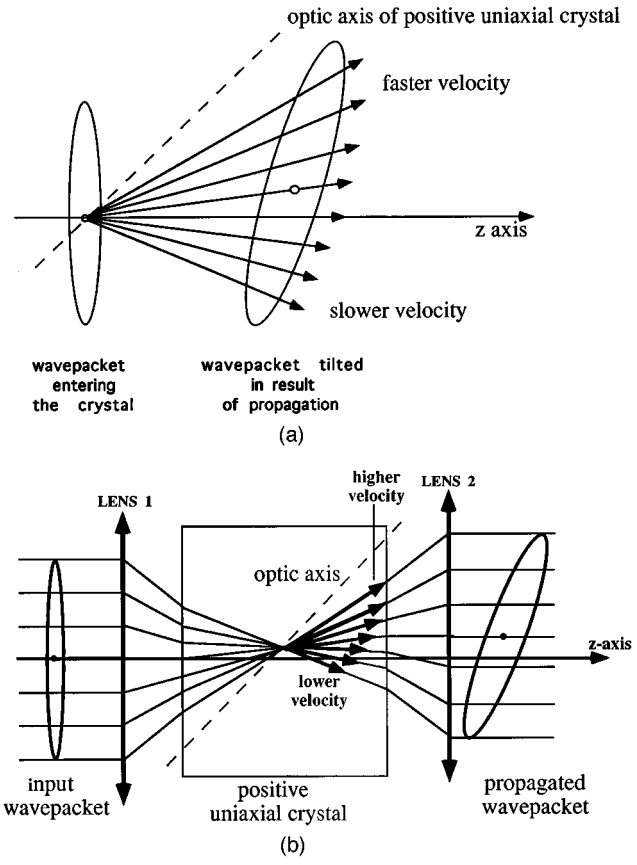

Fig. 1. (a) Schematic representation of a WP propagating in a positive uniaxial crystal. The initial WP is shown on the left. Velocities in the crystal are shown as arrows. The dots in the WP's represent their centers. The propagated WP is tilted, time broadened by dispersion, and moved off axis owing to the walkoff. The effects of diffraction are not shown. (b) Diagram of our experimental situation. The initial WP is shown on the left. Velocities in the crystals are shown as arrows. The dots in the WP's represent their centers. The WP is tilted, time broadened by dispersion, and moved off axis owing to the walkoff. The effects of diffraction are not shown.

beam. Numerical simulation shows that the wave-packet tilt in our crystals should advance one side of the WP by ~20 fs with respect to the other side. When measured with standard intensity correlation (cross correlation) techniques, such a pulse would appear longer, with measured pulse duration depending on the intensity distribution across the beam. Since such measurements yield results integrated over the whole beam cross section, it is difficult to separate the pulse broadening from the pulse tilt. In addition, intensity correlation techniques require high power and are sensitive to the power fluctuations. For this reason we used a linear interferometric technique similar to methods used in Refs. 3–5. However, we used femtosecond-pulse illumination rather than broad-spectrum cw light. The method relies on the fact that the position of maximum contrast in the interference pattern created by two interfering nearly Fourier-limited WP's corresponds to the best time overlap of two WP's. Figure 2 shows the experimental setup that was based on a modified Michelson interferometer and that contained rutile crystals in both arms. A beam from a homemade Ti:sapphire laser operating at 800 nm and generating approximately 30-fs pulses[6] was input into the interferometer, and the interference fringes were recorded. The light polarization was set parallel to the plane of Fig. 2, and the beams propagated as extraordinary rays in both crystals. Arm 2 of the interferometer contained an objective lens L3, which focused the beam into a rutile crystal C2 and a recollimating lens L4 so that the system of lenses with the crystal between them formed a telescope with unit magnification. Each objective consisted of two thin quartz lenses (1.5-mm thickness) to minimize group-velocity dispersion. Arm 1 is identical to arm 2 except for the fact that mirror M1 was mounted on a piezotransducer, which in turn was attached to a computer-controlled submicron-precision translation stage. The interferometer without crystals produced a single fringe-interference pattern. Two identical 1-mm-thick rutile crystals with the optic axis oriented at 45° to the surface of the crystal and oriented as shown in Fig. 2 were used. With the crystals installed the fringe pattern was slightly changed but a single fringe-interference pattern could still be obtained. However, imperfect wave-packet overlap resulted in a fringe pattern limited to a part of the output beam.

The interferometer output beam was split into two beams so the interference pattern could be simultaneously monitored by a TV camera and measured by a silicon photodiode. The photodiode was mounted on a translation stage that moved in the plane of Fig. 2 across the output beam. Thus the photodiode could monitor the interference pattern at different positions across the image. The signal from the photodiode was digitized and recorded in a PC.

Light propagating inside the crystal at different angles to the optic axis experiences angle-dependent phase and group-velocity delays. Light propagating at a small angle to the optic axis of the uniaxial rutile crystal propagates fast whereas light at a large angle to the optic axis propagates slowly both in the sense of phase and group velocity. Once the WP is outside the crystal the propagation vector of the light field ($\mathbf{k}_0$) is normal to the con-

stant phase surface. Moreover, the phase surface reaching the photodiode is well approximated by a local plane-wave surface because the beam is collimated. The direction-dependent difference between the phase and the group velocities experienced by the WP inside the crystal manifests itself as an advance of the fast side of the WP and retardation of the WP at the slow side in respect to the constant phase surface. Hence the constant phase surface provides a convenient reference surface for measurement of the effect. The WP's leaving both arms of the interferometer will be tilted so that they are advanced at the fast side of the WP and retarded at the slow side. For the orientation of the crystals shown in Fig. 2, the slow side of the WP propagating through C1 interferes with a fast side propagating through C2 and vice versa. The resulting tilt of the WP's is illustrated in exaggerated form in Fig. 2 by ellipses drawn with dashed lines. If the time delay for the extreme left and right parts of the WP's were larger than the laser pulse duration, the interference fringes would be visible only in the part of the beam that contained time-overlapping parts of the rotated WP's. The fringes would be visible only in the left part of the beam presented in Fig. 2. Photographs of the fringes taken by the TV camera for different delays between the pulses are presented in Fig. 3. Here the interferometer was intentionally misaligned to produce several fringes parallel to the plane of Fig. 2 for visualization of the effect. Such a misalignment does not introduce any time delay between the left and the right sides of the beam. The location of the high-contrast fringes shift across the beam as the relative delay between the beams changes. In our system the delay was adjusted by moving mirror M1. For all other measurements the interferometer was aligned for a single fringe in the interference pattern. This ensured collinearity of the output beams and made the phase planes of the two interfering WP's parallel.

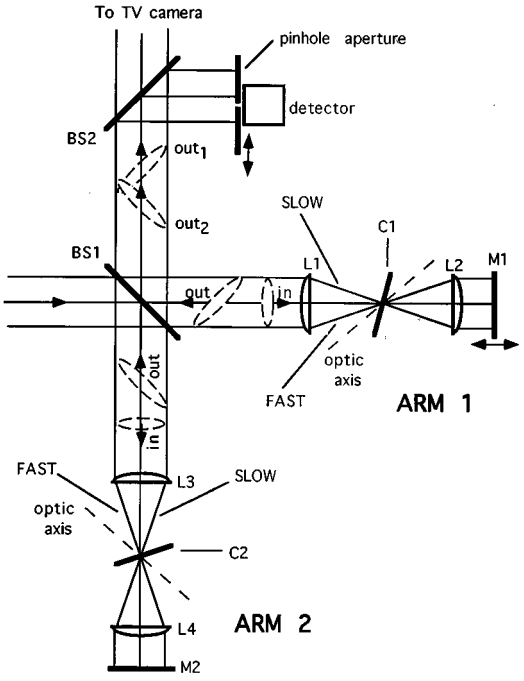

Fig. 2. Michelson interferometer used in the experiment. L1–L4 are lens objectives, M1 and M2 are flat mirrors, C1 and C2 are rutile crystals, and BS1 is a 50% beam splitter. Ellipses drawn with dashes indicate the WP's propagating in the system.

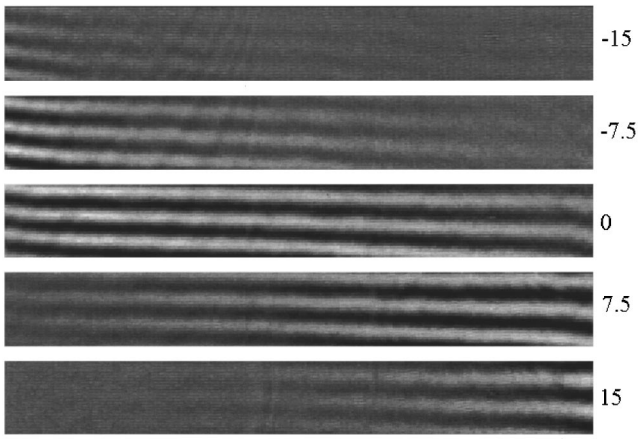

Fig. 3. Set of images of the interference patterns taken by the TV camera for a set of path differences between arm 1 and arm 2. The numbers next to the pictures are positions of mirror M1 in micrometers.

Two effects can potentially obscure the results of the experiments: (a) wave-packet distortions by lenses and plane-parallel plates (crystals) and (b) group-velocity dispersion effects.

(a) In our system lens chromatic aberration was not corrected. This causes wave-packet distortion,[7] but since identical sets of lenses were used in both interferometer arms, wave 1 interfered with identically distorted wave 2, and not only a single fringe interference pattern resulted, but also perfect spatial overlap of the WP's was observed when the system was aligned without crystals.

The time delay of the diverging WP in the plane-parallel slab of a birefringent crystal consists of two separate contributions. One contribution arises owing to the change of the difference between phase and group velocities as a function of direction in the crystal as described in Ref. 1, whereas the other is connected to the geometrical path length of rays in the crystal. The ray propagating in the crystal at right angle to the surface of the crystal has the shortest path, but the path lengths of rays propagating in other directions are longer. The latter effect leads to spatial distortion similar to pulse distortion by lenses[7] but contained in one dimension. The extraordinary ray in our rutile sample with the optic axis at 45° to the surface propagates at a right angle to the surface for an incidence angle equal to ~16° (this incidence angle was used in the experiment). Figure 4 shows the calculated path difference with respect to the central ray for the range of incidence angles used in the experiment. The calculated path difference with respect to the central ray at 16° is nearly symmetric about 16°. The asymmetry is less than one wavelength for the whole angular range. Therefore in our system the geometrical effect can be neglected, and the only contribution to the observed effect comes from the direction-dependent group velocity.

(b) Rutile crystals and other optical elements in the interferometer introduce group-velocity dispersion, result-

ing in pulse broadening. This was compensated by a double-pass negative group-velocity delay line[8] that was placed between the laser and the interferometer. The group-velocity delay line was adjusted by minimizing the duration of the pulse leaving the interferometer. The pulses at the output of the interferometer were nearly Fourier limited, and the position of maximum contrast in the interference pattern corresponded to the best local overlap of the two interfering WP's. It is worth noting that the requirement of Fourier-limited pulses at the output of the interferometer is not very strict. It can be shown that the presence of linear frequency chirp in the output pulses does not alter the time position of the maximum fringe visibility; it simply lowers and broadens the fringe visibility versus the delay curve.

Visibility of fringes versus delay were measured for different transversals of the beam (corresponding to incidence angles from 6° to 26°). Fringe visibility for a given position of the photodiode and a given delay was measured by application of an ac voltage to the piezotransducer to produce slightly more than $\lambda/2$ displacement of mirror M1. This caused the light intensity in the interference pattern to swing over more than one cycle. $I_{\min}$ and $I_{\max}$ intensities were measured, and a standard fringe visibility was calculated. This procedure was repeated for different positions of mirror M1 collecting visibility versus delay curve. Results of the measurements for left, central, and right parts of the beam are presented in Fig. 5(a). Measured values of fringe visibility were slightly below unity, probably because of the use of uncoated optics and imperfect group-velocity-dispersion compensation. Clearly, the area of maximum fringe visibility shifted as the delay varied, indicating that the two output WP's were tilted with respect to each other.

It is worth noting that rotating crystal C2 by 180° with respect to the direction of arm 2 of the interferometer replaces the slow side by the fast side in the beam of this arm. Now, the slow part of the WP from arm 1 interferes with the slow part of the WP from arm 2, and the fast part from arm 1 interferes with the fast part from arm 2. All other delays caused by the optics remain unchanged. Thus both output WP's overlap across the whole cross section of the beam, and the fringe visibility versus delay curves are the same for any position of the detector in the output beam. Figure 5(b) shows data taken with one of the crystals rotated by 180° as described above. In this configuration both WP's were tilted the same way, and they fully overlapped across the beam cross section. As expected, Fig. 5(b) shows the fringes appearing and disappearing simultaneously across the whole beam.

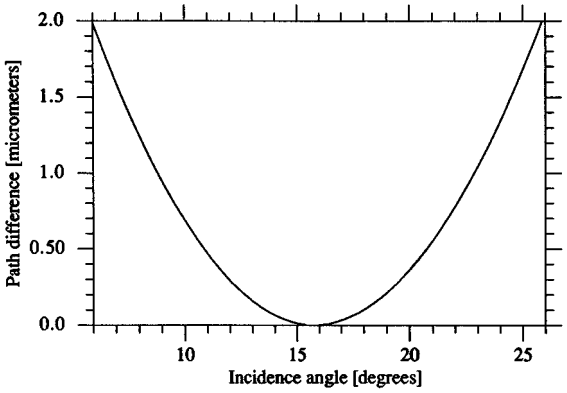

Fig. 4. Calculated path-length difference for the extraordinary ray in a 1-mm-thick rutile crystal with respect to the central ray for the range of incidence angles used in the experiment.

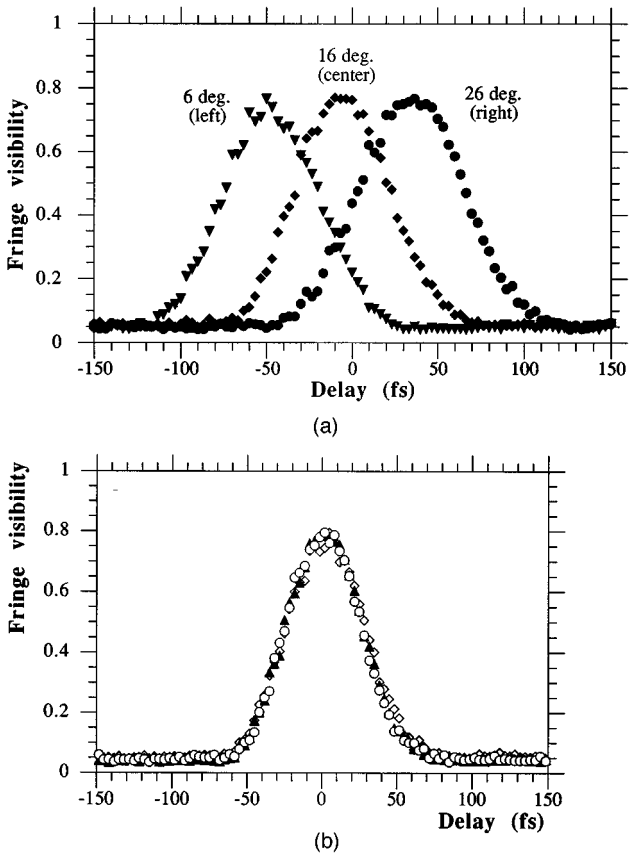

Fig. 5. (a) Visibility of fringes in three different regions of the beam corresponding to incidence angles of 6°, 16°, and 26° (left, central, and right parts of the beam). (b) Visibility of the fringes with one of the crystals rotated by 180° as described in the text. Here the triangles, squares, and circles correspond to the left, center, and right, respectively.

Fringe-visibility curves with crystals oriented to observe wave-packet tilting were measured for several positions in the output beam. The experimental fringe-visibility curves were fitted by Gaussian function and the positions of maxima of the curves were established. Figure 6 shows that the experimental data are in very good agreement with the calculation based on ray tracing assuming rutile refractive indices at 800 nm equal to $n_o = 2.52$ and $n_e = 2.79$.[2] The pulse tilting corresponding to a time difference of ~91 fs between the left and the right parts of the beam (corresponding to incidence angles of 6° and 26°) was measured with precision of ~1 fs by laser pulses of ~30 fs. A single pass through a single crystal would produce 1/4 of the observed effect, i.e., 22.7 fs.

We experimentally confirmed tilting of the femtosecond WP owing to crystal birefringence. Using the linear interferometric method, we were able to establish relative positions of different parts of the WP's with femtosecond precision. The linear method is much more sensitive

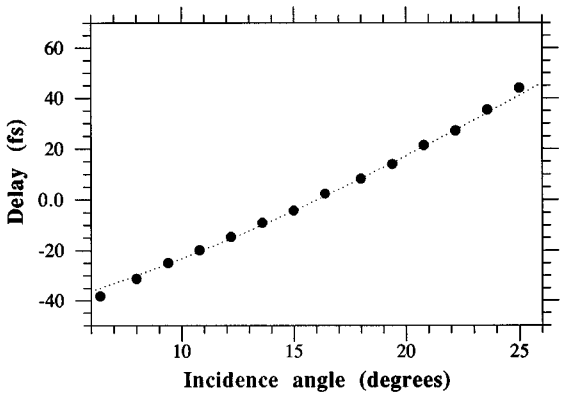

Fig. 6. Calculated (dotted curve) and measured (symbols) time-delay differences versus incidence angle for our experimental configuration.

than the intensity correlation technique; its sensitivity limit is set by the shot noise. Moreover, the linear method is quite insensitive to slow laser-power fluctuations because the quantity measured does not depend on the input power. The method might find applications in the study of other effects involving distorted pulses.

ACKNOWLEDGMENTS

Support of this project by the Presbyterian Foundation, the Center for Laser Research of Oklahoma State University, Allied Signal Inc., KBN grant 2P03B06309 and the Israel Academy of Science is acknowledged.

REFERENCES

1. M. Trippenbach and Y. B. Band, Phys. Rev. Lett. **76**, 1457–1460 (1996); Y. B. Band and M. Trippenbach, J. Opt. Soc. Am. B **13**, 1403–1411 (1996).
2. M. J. Weber, *Handbook of Laser Science and Technology* (CRC, New York, 1986), Vol. 4, p. 233.
3. W. H. Knox, N. M. Pearson, K. D. Li, and C. A. Hirlimann, Opt. Lett. **13**, 574–576 (1988).
4. Z. Bor, Z. Gogolak, and G. Szabo, Opt. Lett. **14**, 862–864 (1989).
5. Z. Bor, K. Osway, B. Racz, and B. Szabo, Opt. Commun. **78**, 109–112 (1990).
6. C. Radzewicz, G. W. Pearson, and J. S. Krasinski, Opt. Commun. **102**, 464–468 (1993).
7. Z. Bor, Opt. Commun. **14**, 119 (1989); Z. L. Horvath and Z. Bor, Opt. Commun. **108**, 333 (1994).
8. R. L. Fork, O. E. Martinez, and J. P. Gordon, Opt. Lett. **9**, 150 (1984).